University of Zurich[UZH]

Zurich Open Repository and Archive
University of Zurich
University Library
Strickhofstrasse 39
CH-8057 Zurich
www.zora.uzh.ch

Year: 2012

PAX2 is an antiapoptotic molecule with deregulated expression in medulloblastoma

Burger, M C ; Brucker, D P ; Baumgarten, P ; Ronellenfitsch, M W ; Wanka, C ; Hasselblatt, M ; Eccles, M R ; Klingebiel, T ; Weller, M ; Rieger, J ; Mittelbronn, M ; Steinbach, J P

Abstract: PAX2 is a paired box transcription factor possessing a fundamental role in the embryogenesis of hindbrain and urinary tract. PAX genes are proto-oncogenes, PAX2 expression may contribute to the pathogenesis of renal cell carcinoma. Because of the expression of PAX2 in the developing hindbrain and its essential role in cerebellar development, it has been hypothesized that PAX2 may also be involved in medulloblastoma tumorigenesis. We investigated the expression pattern of PAX2 and various genes of the neuronal lineage in medulloblastoma and glioma cell lines. We found high expression of PAX2 mRNA and PAX2 protein in medulloblastoma cells and some glioma cell lines independent of their neuronal lineage gene expression signature. Gene suppression of PAX2 decreased the expression of the PAX2 transcriptional target GDNF in Daoy cells and had a profound cytotoxic effect in vitro on Daoy medulloblastoma and T98G glioma cells. Expression of PAX2 was then assessed in two separate medulloblastoma tissue microarrays with a total of 61 patient samples by immunohistochemistry. PAX2 expression was detected in the majority of medulloblastoma samples and correlated with less differentiated histology. Therefore, PAX2 is a biomarker for a more aggressive medulloblastoma phenotype and may represent a novel therapeutic target.

DOI: https://doi.org/10.3892/ijo.2012.1446

Posted at the Zurich Open Repository and Archive, University of Zurich
ZORA URL: https://doi.org/10.5167/uzh-64655
Journal Article
Accepted Version

Originally published at:
Burger, M C; Brucker, D P; Baumgarten, P; Ronellenfitsch, M W; Wanka, C; Hasselblatt, M; Eccles, M R; Klingebiel, T; Weller, M; Rieger, J; Mittelbronn, M; Steinbach, J P (2012). PAX2 is an antiapoptotic molecule with deregulated expression in medulloblastoma. International Journal of Oncology, 41(1):235-241.
DOI: https://doi.org/10.3892/ijo.2012.1446

PAX2 is an antiapoptotic molecule with deregulated expression in medulloblastoma.

Burger MC*, Brucker DP*, Baumgarten P, Ronellenfitsch MW, Nordhammer C, Hasselblatt M, Eccles MR, Zernicka-Goetz M, Busslinger M, Klingebiel T, Weller M, Rieger J, Mittelbronn M, Steinbach JP.

Abstract

PAX2 is a homeobox transcription factor with fundamental roles in the embryogenesis of hindbrain and urinary tract. *PAX* genes are protooncogenes and it has been suggested that *PAX2* contributes to the pathogenesis of renal cell carcinoma. Due to their expression in the developing hindbrain and their essential role in cerebellar development, it has been hypothesized that *PAX2* and *PAX5* may be involved in medulloblastoma tumorigenesis. Interestingly, *PAX5* is re-expressed in most medulloblastomas. However, we have previously shown that overexpression of *Pax5* is not sufficient for medulloblastoma formation in mouse models. We here investigated the expression pattern of *PAX2* and several other genes of neuronal lineage in medulloblastoma and glioma cell lines. We found high expression of *PAX2* mRNA and PAX2 protein in medulloblastoma cells and some glioma cell lines independent of neuronal differentiation. Gene suppression of *PAX2* decreased the expression of the *PAX2* transcriptional target GDNF and had a profound cytotoxic effect *in vitro*. Expression of *PAX2* was then assessed in two separate medulloblastoma tissue microarrays with a total of 61 patient samples by immunohistochemistry. *PAX2* expression was detected in the majority of medulloblastoma samples and was correlated with less differentiated histology. Therefore, *PAX2* is a biomarker of more aggressive medulloblastoma and may represent a novel therapeutic target.

208 words

Introduction

The paired box transcription factor gene family has been well characterized both in human (*PAX*) and mouse (*Pax*) and consists of nine genes in the human genome which encode the corresponding transcription factors (PAX/Pax)[1]. Every *PAX* gene encodes one transcription factor which contains the characteristic DNA binding paired domain. The *PAX* genes can be divided into four subgroups according to sequence homologies: *PAX1/PAX9, PAX2/PAX5/PAX8, PAX3/PAX7* and *PAX4/PAX6*[2, 3].

PAX genes, like other developmental control genes, are proto-oncogenes[4, 5]. They serve to orchestrate the expression of target gene responses that enable proliferation and suppress apoptosis in their target tissues[6]. The expression patterns of *PAX* genes are therefore tightly regulated both in a spatial and temporal manner during embryonal development. *PAX2*, in particular, is important for hindbrain and renal development. Interestingly, in hindbrain development, the closely related paralogous *PAX* genes (*PAX2*, *5* and *8*), can compensate for the loss of one another and a major cerebellar phenotype occurs when two alleles are lost, i.e., five out of the six alleles are necessary[7, 8]. In general, *PAX* genes are downregulated in differentiated tissues[9, 10]. In particular, expression of *PAX2*, *PAX5* and *PAX8* is suppressed in postnatal hindbrain. Nevertheless, expression of some *PAX* genes is maintained postnatally in specific tissues. *PAX4* and *PAX6* are expressed in exocrine cells of the pancreas[11-13], *PAX6* is expressed in the cerebellum[14] and *PAX8* in the thyroid gland[11, 15]. The suppression of p53 expression by PAX2, PAX5 and PAX8 by binding to the 5´ regulatory unit of the human p53 gene is one example of the mechanisms involved in control of growth and cell death by *PAX* genes[16].

In line with their biological functions, deregulated expression of *PAX* genes can drive the development of tumors in children and adults. Specifically, fusion genes involving *PAX3* or *PAX7* cause alveolar rhabdomyosarcoma[17-19]. An oncogenic fusion gene involving the IG

enhancer and *PAX5* has been found in malignant B-cell lymphomas[20, 21]. *PAX8* can also be involved in a translocation which results in the PAX8-PPARγ fusion protein, which is frequently found in follicular thyroid carcinoma[22]. Elevated *PAX2* expression has been found in cystic and hyperproliferative disorders of the kidney, possible predecessors of renal cell carcinoma[10, 23, 24]. Genetic alterations like point mutations and translocations have been described in kidney hypoplasia and the coloboma-kidney syndrome[25-28]. A high proportion of primary renal cell carcinomas expressed *PAX* [29]. It is known that an elevated expression of *PAX2* mitigates cisplatin-induced cytotoxicity and blocks caspase-2 induced apoptosis in ACHN and CAKI-1 renal carcinoma and human embryonic kidney 293 (HEK293) cells[30, 31]. Accordingly, inhibition of *PAX2* with specific siRNAs in the cell lines EJ (bladder carcinoma) and IGROV-1 (ovarian carcinoma) increased the rate of apoptosis thereby lowering the proliferation rate[32]. The same effect was seen in immortalized rat proximal tubulus cells[33]. Due to the expression pattern of *PAX2*, *PAX5* and *PAX8*, particular interest has been generated in these genes as candidate genes involved in the genesis of medulloblastoma, the most common malignant embryonal brain tumors that originates from the hindbrain. Interestingly, *PAX5* is re-expressed in most medulloblastomas in contrast to differentiated cerebellum tissue[14]. However, overexpression of *Pax5* by retroviral transfer to embryonic neuroectodermal precursor cells or in the granule cell layer of engrailed2-*Pax5* transgenic mice was not sufficient for medulloblastoma formation[34]. We therefore here investigated the expression pattern of *PAX2* and *PAX8* in addition to *PAX5* in medulloblastoma cells and compared it to their expression in glioma cells, in which expression of *PAX5* has been shown to correlate inversely with the expression of p53[16]. We found high expression of *PAX2* in medulloblastoma cells and the majority of medulloblastoma samples from two separate tissue microarrays. Gene suppression of *PAX2* had a profound cytotoxic effect *in vitro*.

Material and methods

Cell culture

Daoy medulloblastoma cells were a gift from T. Pietsch (Bonn, Germany). The human malignant glioma cell lines were kindly provided by N. de Tribolet (Lausanne, Switzerland). The murine glioma cell line SMA560 was a gift of D. D. Bigner (Durham, NC, USA). The immortalized astrocytic cell line SV-FHAS was kindly provided by A. Muruganandam (Ottawa, Canada). All cells were maintained in DMEM containing 10% fetal calf serum (Biochrom KG, Berlin, Germany), 2mM glutamine and 100IU/ml penicillin/100µg/ml streptomycin (Life Technologies, Karlsruhe, Germany).

Glioma cell lines were stably transfected by lipofection using FuGene6 (Roche, Mannheim, Germany). The plasmids encoding human *PAX2b* or *PAX2c* (pCMV/PAX2-N1 and pCMV/PAX2-N3 respectively plus the empty control vector pHN/CMV) were kindly provided by M. Eccles (Otago, New Zealand)[35, 36]. The plasmid encoding murine *Pax2* (pmPax2/334 plus the empty vector pKW10) was kindly provided by M. Busslinger (Vienna, Austria). At 48 h after transfection, the cells were shifted to medium supplemented with G418 sulphate (1 mg/ml) or puromycin (2 mg/ml). For all experiments, pooled transfectants rather than single clones were used.

For transient gene suppression of human *PAX2*, a small interfering RNA (siRNA) was employed (Thermo Fisher Scientific, Dharmacon Products, Lafayette, CO, USA). The following sequences targeting the human *PAX2* coding region were used: d1: 5′-AAACUGUCCACACCACUCUUU-3′; d2: 5′-UCUGAUUUGAUGUGCUCUGUU-3′. A predesigned scrambled siRNA was used as control (Thermo Fisher Scientific, Dharmacon Products, Lafayette, CO, USA). For transient siRNA transfections Metafectene Pro was employed according to the protocol with a final siRNA concentration of 50nM and 0.33µl Metafectene Pro in 100µl transfection medium per well for 96-well plates.

Cell growth was assessed by crystal violet staining as previously described[37]. Cell viability was analysed by lactate dehydrogenase (LDH) release assays[38]. For the detection of chemotherapy-induced cell death, the cells were plated on 96 well plates (Falcon, Becton-Dickinson) at 1.5 x 10^4/well and allowed to attach overnight. Then the cells were incubated with chemotherapeutics for 72 hours in serum-free medium and stained with crystal violet. Alternatively cell viability was measured by flow cytometry: First cells were washed with ice-cold PBS, stained with 5µg/ml propidium iodide (PI) in PBS and then analysed by flow cytometry. For cell cycle analysis, detached cells were harvested from the supernatant by centrifugation and added to the non-detached cells harvested by trypsination. The cells were washed with phosphate-buffered saline, fixed in 70% ice-cold ethanol, centrifuged, washed with phosphate-buffered saline again, stained with propidium iodide (50 µg/ml) diluted in phosphate-buffered saline containing RNase A (100 µg/ml) and subjected to flow cytometric analysis of DNA content using Dako CyAn Cytometer. Percentages of sub-G1 cells were calculated using the Dako Summit software (Dako, Glostrup, Denmark).

Real-time PCR

RNA was isolated using the RNeasy Mini Kit (Qiagen, Hilden, Germany). Superscript II RT (Gibco, Life Technologies, Carlsbad, CA, USA) was employed for cDNA synthesis. cDNA amplification was monitored using SYBR Green chemistry (ABgene, Epsom, UK) on the ABI PRISM 7000 Sequence Detection System (Applied Biosystems, Weiterstadt, Germany). The conditions for all PCR reactions were as follows: 40 cycles of 95°C for 15s and 60°C for 1 min, using the following specific primers (forward and reverse): 18S: 5′-CGGCTACCACATCCAAGGAA-3′, 5′-GCTGGAATTACCGCGGCT-3′; DLX1: 5′ TGGAATCCGAACTCCTCATC-3′, 5′- TCACATCAGTTGAGGCTGCT-3′; EMX2: 5′-AGCTTCTAAGGCTGGAACACGC-3′; 5′- TACCTGAGTTTCCGTCAGGCTG-3′; hASH1: 5′-

AGGAGCTTCTCGACTTCACCAA-3′; 5′-ATCACCCTGCTTCCAAAGTCC-3′; NGN2: 5′-AGAGCCAACTAAGATGTTCGTCAAA-3′; 5′- CCGATCCGAGCAGCACTAAC-3′; OLIG2: 5′-AACTCCTCCACGTGCTTCCTG-3′; 5′- CGGTGCGATCAGAGGAAGG-3′; PAX2: 5′-TGTGGACAGTTTGCGGAAGCA-3′, 5′-TGATGTGCTCTGATGCCTGGAA-3′; PAX5: 5′-AAGCGCAAGAGAGACGAAGGT-3′, 5′-TGAACAAGTCTCCCCGCATC-3′; PAX6 : 5′-GACTTCGGTGCCAGGG-3′ , 5′-TGGTATTCTCTCCCCCTCCTT-3′; PAX8 : 5′-ACAAACGCCAGAACCCTACCAT-3′, 5′-TTAATGGAGCTGACACTGGGCA-3′.

Relative mRNA levels were calculated by $2^{(-\text{Delta Delta C(T)})}$ Method[39].

Immunoblot analysis

Cells were washed with ice-cold PBS and harvested into ice-cold PBS containing protease inhibitors. Cellular lysates were prepared as described[40] and subjected to SDS-PAGE analysis. Equal loading was ascertained by Ponceau S staining. Membranes were probed with polyclonal rabbit anti-human PAX2 antibodies (Cat. No. 71-6000, Invitrogen Corporation, Life Technologies, Carlsbad, CA, USA) or goat anti-ß-actin (SC-1616, Santa Cruz Biotechnology, Santa Cruz, CA, USA). The secondary anti-rabbit and anti-goat antibodies were purchased from Santa Cruz Biotechnology. Enhanced chemiluminescence (ECL+) (Amersham, Little Chalfont, UK) was used for detection.

Induction of hypoxia

Hypoxia was induced by incubating cells in Gas Pak pouches for anaerobic culture (Becton Dickinson, Heidelberg, Germany)[40]. Briefly, the cells were plated on 96 well plates at 2 x 10^4/well and allowed to attach overnight. Then the cells were incubated in serum-free DMEM without glucose (Gibco BRL, Basel, Switzerland) adjusted to 2 mM glucose under normoxia

or hypoxia for the indicated time periods. Equal cell densities were ensured by crystal violet staining when comparing cells expressing vehicle and *PAX2b*, *PAX2c* or murine *Pax2*. Cell death was assessed by means of LDH release assay.

Animal studies

VMdK mice were anesthetized and placed in a streotactic fixation device (Stoelting, Wood Dale, IL, USA). 5,000 SMA560 cells stable transfected with vehicle or murine *Pax2*, were injected into the right striatum. The mice were sacrificed when developing neurological symptoms. All animal research was carried out in accordance with the law for treatment of animals in Germany and approved by the local authorities (N3/03, Regierungspräsidium Tübingen, Germany).

Human tissue specimens

We investigated two independent tissue microarrays containing medulloblastoma specimens of 61 patients and 3 normal appearing cerebellar specimens from the tumor banks of the departments of neuropathology of the University of Frankfurt (n=18) and Münster (n=43). All tissues were evaluated by at least two neuropathologists according to the current classification of tumours of the central nervous system[41] using routine HE, reticulin and immunohistochemical stainings including antibodies against Ki-67, GFAP, MAP2, NeuN, synaptophysin and vimentin.

Cell pellets for immunocytochemistry

The human medulloblastoma and glioma cell lines cells were maintained in DMEM containing 10% FCS and penicillin (100 IU/mL)/streptomycin. 50 million cells of each cell line were detached using Accutase, centrifuged for 5 min at 1000 U/min. Cell pellets were fixed in 4% buffered formalin (pH 7.4) for 24 paraffin-embedded afterwards.

Immunohistochemistry

All human tissue specimens were fixed in 4% buffered formaline (pH 7.4), embedded in paraffin, cut with a microtome (3µm thickness) and placed on SuperFrost Plus slides (Microm International, Walldorf, Germany). For immunohistochemistry, the following antibody was used: polyclonal rabbit anti-human PAX2 (Invitrogen Corporation, CA, USA). Establishment of the immunostainings was performed on full mount sections whereas for statistical analysis a tissue micro array (TMA) consisting of all human medulloblastoma samples was investigated. Tissue labelling for PAX2 was performed using DiscoveryXT immunohistochemistry system (Ventana, Strasbourg, France). A cell conditioning pretreatment was performed for 44 min. After a 4 min blocking step with inhibitor D (Ventana, Strasbourg, France) the primary antibody was applied at 1:50 for 32 min followed by a 28 min incubation with one drop of I-View-Biotin Ig (Ventana). An avidin and a biotin blocker was applied to the samples for 4 min. For diaminobenzidine (DAB) visualization, the sections were incubated with one drop of I-View SA-HRP for 16 min and then with DAB/H_2O_2 for additional 8 min. The sections were finally incubated with a copper enhancer (Ventana) for 4 min, washed, counterstained with hematoxylin and mounted.

Immunocytochemistry

All cell pellets were cut with a microtome (3µm thickness) and placed on SuperFrost Plus slides (Microm International, Walldorf, Germany). Immunocytochemical PAX2 staining was performed using the same protocol as for the immunohistochemical analysis. Additionally cell pellets were stained for GFAP, MAP2, NeuN, vimentin and synaptophysin.

Tissue microarray evaluation

Immunostained sections were evaluated by 2 examiners (PB and MM). A semi-quantitative score including staining intensity and frequency similar to commonly used scores in routine pathology was applied[42]**.** The frequency score ranged from 0-4 (Score=0, 0-1%; score=1, 1-10%; score=2, 10-25%; score=3, 25-50% and score=4, >50% of all cells showing a positive staining). The intensity score ranged from 0-3 (0, no staining; score=1, weak staining; score=2, moderate staining and score=3, strong staining). The two results for staining intensity and frequency were multiplied, so that a "Multi-Score" reflected both.

Statistical analysis

Where indicated, analysis of significance was performed using the two-tailed Student *t* test with $P < 0.05$ considered significant and $P < 0.01$ considered highly significant (Excel; Microsoft, Seattle, WA, USA). Evaluation of survival patterns in mice bearing intracerebral gliomas was performed by the Kaplan-Meier method.

Contingency analysis for PAX2 expression scores derived from the the tissue microarray studies according to histomorphological subtypes was performed followed by Pearsons Chi square test. JMP IN 8.0 (SAS Institute, Cary, NC, USA) was used for statistical analysis.

Results

PAX2 is highly expressed in Daoy human medulloblastoma cells and some malignant human glioma cell lines.

To investigate the pattern of expression of *PAX2*, *PAX5* and *PAX8* we first screened the human medulloblastoma cell line Daoy and a panel of established human malignant glioma cell lines by means of quantitative RT-PCR (qPCR). High *PAX2* mRNA levels were found in Daoy cells as well as in the glioma cell lines T98G and A172 **(Fig. 1A).** These results were confirmed by western blot analysis and immunohistochemistry of cytopellets **(Fig. 1A)**. In contrast, *PAX5* mRNA expression was restricted to the medulloblastoma cell line Daoy **(Fig. 1B)**. *PAX8* was not detectable in Daoy cells, but five out of twelve glioblastoma cell lines showed *PAX8* mRNA expression **(Fig. 1C)**. We also investigated the mRNA expression of *PAX6*, whose expression in normal human brain, gliomas and medulloblastomas has been described previously[14, 43] and confirmed low levels of expression of *PAX6* in Daoy cells, all glioma cell lines as well as the immortalized astrocytic cell line SV-FHAS (data not shown).

Overexpression of PAX2 has no effect on proliferation rate or sensitivity against chemotherapeutic agents and hypoxia in human LNT-229 glioma cells.

Because overexpression of *PAX2* has a well characterized oncogenic function in renal carcinoma[32] we introduced *PAX2* into non-expressing glioma cell lines in order to conduct functional experiments. Stable transfectants were established in A172, LN-18, LNT-229 and U88MG cells with the *PAX2* isoforms *PAX2b* and *PAX2c* or the control vector coding for neomycin resistance (neo). Representative western-blots from LNT-229 *PAX2b* and *PAX2c* cells are shown in **Fig. 2A**. However, in contrast to published effects in some other cell

lines[30, 32], no effect on proliferation **(Fig. 2B)** or sensibility against the chemotherapeutic drugs cisplatinum **(Fig. 2C)** and vincristin **(Fig. 2D)** were found in the transfectants as assessed by crystal violet assay. These experiments also were performed without FCS and with cell densities of 500 and 5,000 cells per well (data not shown).

Because it is increasingly recognized that in the glioblastoma microenvironment cell death is mainly necrotic and hypoxia resistance is highly relevant for therapy, we also investigated the effect of *PAX2* overexpression in a paradigm of hypoxia-induced cell death that closely mimics the mode of cell death observed in vivo[44]. However, there was no significant difference in hypoxic cell death in LNT-229 *PAX2* cells compared to neo cells **(Fig. 2E)**. Under normoxic conditions, the rates of spontaneous cell death were low in both *PAX2* and neo cells **(Fig. 2F)**. Immunocytochemistry of cell pellets for neuronal and glial markers (GFAP, vimentin, NeuN, synaptophysin and MAP2) did not reveal an effect of *PAX2* overexpression in LN-18, LNT-229 and T98G glioma cell lines or a difference between glioma cell lines positive for *PAX2* versus those lacking *PAX2* expression (data not shown).

Stable Pax2 overexpression has no effect on proliferation rate or sensitivity against chemotherapeutic agents and hypoxia in murine SMA560 glioma cells.

Because some oncogenic properties are only evident in the in vivo situation, the syngenic orthotopic mouse model of SMA560 glioma cells in VMDk mice was employed. After transfection of murine *Pax2* into SMA560 mouse glioma cells stable overexpression was achieved (puro). Additionally to the amount of *Pax2* already being expressed intrinsically further *Pax2* expression is seen at the 47kDa band in *Pax2* transfected cells. The unspecific bands at 36 and 42kDa respectively do not change in intensity compared to puro control cells **(Fig. 3A)**. In vitro, growth curves **(Fig. 3B)**, chemosensitivity **(Fig. 3C, D)** and susceptibility towards hypoxia **(Fig. 3E, F)** were unaltered by *Pax2* similar to the results with human

glioma cell lines. We then compared symptom free survival of syngenic VMDk mice after intracranial inoculation of 5,000 SMA560 cells stably transfected with *Pax2* versus puro control cells. However no difference in symptom free survival between tumor implants of the two groups could be observed **(Fig. 3G)**. To rule out a differing ability of the SMA560 puro versus *Pax2* transfected cells to engraft, a clonogenity assay has been performed. 500 cells per well were seeded into a six well plate and incubated for 96 hours. We demonstrated that the same amount of cells adhered to the bottom of the well and were able to form vial colonies (data not shown).

Efficient and specific gene suppression by PAX2 targeted siRNAs d1 and d2 of PAX2 in Daoy and T98G cells.

Transient transfection of Daoy and T98G cells with *PAX2* targeted siRNA *d1* and *d2* compared to *scr* control siRNA, transfection or growth medium alone was performed.
The specificity of the siRNAs was demonstrated by co-suppression of the *PAX2* target gene GDNF[45] as well as *PAX2* itself in Daoy medulloblastoma cells stably overexpressing *PAX2b* **(Fig. 4A, B),** while GFAP, nestin, NSE and vimentin which are not known to be *PAX2* targets were not regulated (data not shown). As in Daoy cells rapid cell death was occurring following *PAX2* downregulation we were not able to show the effect on PAX2 protein level in this cell line. Instead we employed the glioma cell line A172, where the effect on cell survival was less pronounced and the bladder carcinoma cell line EJ[32] to show the effect on PAX2 protein level. Efficient gene suppression in these two cell lines was demonstrated by western blot analysis **(Fig. 4C).**

Gene suppression of PAX2 induces cytotoxic effects in Daoy and T98G cells.

Transient transfection of Daoy cells with *PAX2* targeted siRNA *d1* and *d2* compared to *scr* control siRNA, transfection or growth medium alone had profound cytotoxic effects as shown by crystal violet assay and phase contrast photography **(Fig. 5A, B)**. Flow-cytometric analysis after PI-staining demonstrated an elevated rate of cell death occurring in cells treated with *PAX2* specific siRNA. Cell Cycle analysis employing flow cytometry showed an elevated sub-G1 peak indicating apoptosis as well as a decreased number of cells in S- and M-phase **(Fig 5C)**. A similar effect was observed in T98G malignant human glioma cells **(Fig. 5D-F)**.

PAX2 expression is restricted to basket cells in the normal cerebellum and increases with the degree of malignancy in medulloblastomas.

Because the biologic function of *PAX2* in hindbrain development and the published data on deregulated *PAX5* expression in medulloblastomas as well as our in vitro data strongly suggested a role for *PAX2* in medulloblastomas, we investigated expression of PAX2 protein in medulloblastoma samples from two separate tissue microarrays.

We found that in the normal cerebellum, *PAX2* expression was largely absent. However, basket cells commonly had nuclear *PAX2* expression **(Fig. 6A)**. In medulloblastomas, nuclear *PAX2* expression significantly increased with a less differentiated histomorphological phenotype. While virtually all highly differentiated desmoplastic/nodular medulloblastomas remained *PAX2* negative **(Fig. 6B)**, intermediate nuclear *PAX2* levels were observed in the classic subtype **(Fig. 6C)**. The medulloblastoma with the least differentiated phenotype, mainly the anaplastic subtype, strongly exhibited nuclear *PAX2* expression **(Fig. 6D)**. The statistical analysis of *PAX2* expression related to the medulloblastoma subtypes revealed significant differences ($p<0.005$ in Pearsons Chi square test) showing highest *PAX2* levels in medulloblastomas with the lowest histological degree of differentiation and lowest levels in medulloblastomas with higher differentiated morphology **(Fig 6E)**.

PAX2 expression in gliomas: in silico analyses and correlation with markers of neuronal lineage differentiation.

In contrast to medulloblastoma, the expression of *PAX2* was observed in only a small minority of glioma cell lines. To elucidate possible mechnisms of *PAX2* expression in gliomas, we followed a candidate gene approach and did in silico analyses of glioma mRNA profiling datasets. With the candidate gene approach, we tested the hypothesis that *PAX2* was part of a neuronal signature. Therefore expression of markers known to be involved in neuronal differentiation was investigated in the panel of glioma cell lines, Daoy cells and SV-FHAS cells by qRT-PCR. The data are summarized in **Table 1**. While several of the neuronal markers were highly expressed in gliomas congruent with the increasing awareness of neuronal features in gliomas[46], no correlation of *PAX2* with these markers became apparent. We also established immunohistochemistry on cell pellets of Daoy medulloblastoma and the twelve glioma cell lines as well as the stable *PAX2* transfectants used in our study to assess GFAP, MAP2, NeuN, vimentin and synaptophysin protein expression. However, we observed no difference between *PAX2* positive and negative cell lines or between *PAX2* overexpressing cell lines and their controls (data not shown). *In silico* analyses were performed with the Oncomine registry. According to the Pomeroy gene expression analysis, *PAX2* was 1,889 fold upregulated in classic medulloblastoma samples compared to normal cerebellum probes. GDNF as a *PAX2* target gene was upregulated 2,569 fold in classic medulloblastoma samples (**Fig. 5B**). In gliomas, no significant correlation with neuronal markers defining subclasses of high-grade glioma[46] was apparent. Moreover, *PAX2* was not inversely correlated with p53 mRNA levels (data not shown).

Discussion

Our study demonstrates that *PAX2* is aberrantly expressed in medulloblastoma and glioma cell lines. In particular, the medulloblastoma cell line Daoy expressed *PAX2*, *PAX5* and *PAX6* but not *PAX8*. Out of twelve glioma cell lines two aberrantly expressed *PAX2*, while five others showed *PAX8* expression in a complementary pattern **(Fig. 1)**. Only five glioblastoma cell lines tested neither expressed *PAX2* nor *PAX8*. This is noteworthy, since it has long been established that the three members of the paralogous *PAX2/5/8* group can compensate for each other in the embryogenesis of the midbrain and cerebellum[47] as well as the inner ear development[48]. Interestingly, in *PAX2* negative cell lines, *PAX2* overexpression did not enhance growth, reduce sensitivity against the chemotherapeutic agents cisplatin and vincristine or alter resistance towards hypoxia **(Fig. 2)**. Neither was asymptomatic survival time of syngenic VMdK mice after intracerebral inoculation with SMA560 cells affected by transfection with murine *Pax2* **(Fig. 3G)**. In contrast, by transiently transfecting Daoy medulloblastoma and T98G glioma cell line with *PAX2* specific siRNA molecules we could induce a high level of cell death and a marked effect on proliferation **(Fig. 5)**. This suggests that only the subgroup of tumors which aberrantly maintains PAX2 expression benefits from its antiapoptotic functions whereas the other group relies on alternative mechanisms to evade cell death. It is intriguing to speculate about different tumor stem cell populations with or without PAX2 gene expression as the mechanism of this dichotomy, but there are no data available to test this hypothesis. *PAX2* expression may also serve to compensate for *PAX6* expression and its known tumor suppressor properties, since it has been shown that *Pax2* and *Pax6* repress each other and their target genes[49] and we found *PAX6* expression in Daoy cells and all 12 glioma cells investigated **(Table 1)**.

The cyototoxic effect of PAX2 gene expression in the PAX2-dependent cell lines is congruent with other work demonstrating a potent antiapoptotic function of PAX proteins in some

melanoma, ovarian, bladder and prostate carcinoma cell lines[32, 50-52]. The specifity of the *PAX2* knockdown is supported by its effect on GDNF, a known target gene of *PAX2*, which is suppressed by *PAX2* siRNA **(Fig. 4)**. *In silico* analysis of the Oncomine registry demonstrated that *PAX2* expression is elevated in medulloblastoma compared to normal cerebellum. However, neither our analysis of candidate genes (Table 1) nor *in silico* analysis (data not whown) were able to identify a neuronal signature correlating with *PAX2* expression. Therefore, there is not an obvious role of PAX genes in the evolution of the neuronal phenotype in gliomas.

Finally, to explore the clinical value of *PAX2* as a marker of medulloblastoma, we investigated the expression of PAX2 protein in two tissue microarrays (TMA) containing 61 medulloblastoma samples. The TMA analysis confirmed aberrant *PAX2* expression in medulloblastoma samples, while in normal cerebellum *PAX2* expression was restricted to basket cells **(Fig 6 A-D)**. Importantly, the expression of *PAX2* was associated with histomorphological dedifferentiation, as medulloblastomas with the lowest histological degree of differentiation showed higher *PAX2* expression than medulloblastomas with better differentiation **(Fig. 6 E)**. This is a finding of considerable interest. Therefore, the prognostic and predictive value of PAX2 expression should be validated in prospective studies of medulloblastoma.

In summary, *PAX2* represents a biomarker of more aggressive medulloblastoma and may have potential as a novel therapeutic target.

Figure legends

Fig. 1. PAX2 is highly expressed in Daoy human medulloblastoma cells and some malignant human glioma cell lines.

mRNA from Daoy medulloblastoma cells and a panel of 12 glioma cell lines plus SV-FHAS was investigated for expression of *PAX2* **(A)**, *PAX5* **(B)** and *PAX 8* **(C)** mRNA by RT-quantitative PCR. *PAX2* expression on the protein level was confirmed by western-blotting and immunohistochemistry **(A)**.

Fig. 2. Proliferation and sensitivity against chemotherapeutic agents and hypoxia are not affected by overexpression of PAX2 in human LNT-229 glioma cells.

(A) Stable *PAX2* expression after transfection of vectors coding for *PAX2b* and *PAX2c* was verified by western-blotting. **(B)** Growth rate of LNT-229 cells overexpressing *PAX2b* or *PAX2c* compared to neo control cells as measured by crystal violet assay and normalized to the time point 24 hours after seeding. Sensitivity of LNT-229 cells overexpressing *PAX2b* or *PAX2c* compared to neo control cells against different concentrations of the chemotherapeutic agents cisplatin **(C)** and vincristin **(D)** 72 hours after addition. Hypoxia-induced cell death in LNT-229 cells overexpressing *PAX2b* or neo control cells after 16 hours of hypoxia (0,1% oxygen, 20,000 cells per well in a 96-well plate) **(E)** compared to normoxia **(F)**, LDH release assay.

Fig. 3. Stable Pax2 overexpression does not alter survival in syngenic mice carrying intracranial SMA560 glioma cell grafts.

(A) Stable *Pax2* over-expression after transfection of vectors coding for murine *Pax2* was verified by western-blot. **(B)** Growth rate of SMA560 cells overexpressing *Pax2* compared to puro control cells as measured by crystal violet assay and normalized to the time point 24

hours after seeding. Sensitivity of SMA560 cells overexpressing *Pax2* compared to puro control cells against different concentrations of the chemotherapeutic agents cisplatin **(C)** and vincristin **(D)** 72 hours after addition. LDH release of SMA560 cells overexpressing *Pax2* or puro control cells after 16 hours of hypoxia (0,1% oxygen, 20,000 cells per well in a 96-well plate) **(E)** compared to normoxia **(F)**. Survival time of VMdK mice inoculated with SMA560 cells overexpressing *Pax2* compared to puro control cells **(G)**.

Fig. 4. Efficient and specific gene suppression by PAX2 targeted siRNAs d1 and d2 in Daoy and T98G cells.

(A) mRNA from Daoy cells overexpressing *PAX2b* and cotransfected with *d2 PAX2* specific or *scr* scrambled siRNA was investigated for the level of *PAX2* expression. **(B)** Specifity was verified by determination of mRNA expression of GDNF, a known target gene of *PAX2*. **(C)** *PAX2* downregulation by *d1* and *d2 PAX2* specific siRNAs compared to *scr* scrambled siRNA in A172 glioma cells A172 and EJ bladder carcinoma cells shown by western-blot. See top lane for PAX2 at 47kDa and bottom lane for actin at 45kDa.

Fig. 5. Gene suppression of PAX2 induces cytotoxic effects in Daoy and T98G cells.

Effect of *PAX2* specific siRNAs *d1* and *d2* compared to scrambled siRNA (*scr*), Metafectene Pro transfection reagent (MF) or growth medium alone (VM) on Daoy **(A)** and T98G **(D)** cells as shown by crystal violet assay. Light-microscopic aspect of Daoy **(B)** and T98G **(E)** cells transfected with *PAX2* specific siRNA molecules (*d2*) compared to scrambled siRNA (*scr*) or Metafectene Pro transfection reagent (MF). Effects of transfection with *d2* or *scr* siRNA on cell viability and proliferation measured by propidium iodide staining and flow cytometry in Daoy **(C)** and T98G cells **(F)**. Elevation of *PAX2* expression by the factor of 1,889 (p=0.002) and GDNF as a *PAX2* target gene by the factor of 2,569 (p=3.12E-4) in classic medulloblastoma samples compared to normal cerebellum probes according to

Oncomine registry (Pomeroy brain dataset) **(G)**. Expression levels are normalized to the log2 median-centered intensity of the gene expression arrray. Boxed areas display the 75th percentile, the median and the 25th percentiles. Error bars delineate the 90th and 10th percentiles while the dots specify the maximum and minimum values.

Fig. 6. PAX2 expression increases with the degree of malignancy in medulloblastomas.

(A) *PAX2* immunohistochemistry in the normal cerebellum revealed that only basket cells (arrows) exhibit a strong nuclear *PAX2* expression while other neuronal cells such as Purkinje cells (inset – arrowhead) or granular cells (inset – asterisk) remained completely negative. *PAX2* expression in medulloblastomas varied according to the degree of differentiation showing lowest levels in desmoplastic **(B)** or nodular subtypes, intermediate levels in the classic medulloblastoma subtype **(C)** and strongest *PAX2* expression in undifferentiated anaplastic **(D)** medulloblastomas (asterisk indicating tumor necrosis). **(E)** Statistical analysis of nuclear *PAX2* expression according to the medulloblastoma subtype using contingency analysis showing the Multi-score proportions of *PAX2* expression in medulloblastoma specimens. Ordinal scaled response variable (Multi-Score) and nominal explanatory variable (amount of specimens) were analysed with a contigency analysis ($p<0.005$ in Pearsons Chi square test). The area of one box is corresponding to the amount of specimen falling in the equivalent specific group of Multi-score analysis of *PAX2* expression.

Table 1. Homeobox and helix-loop-helix transcription factors in glioblastoma and medulloblastoma.

Expression pattern of homeobox or helix-loop-helix transcription factors DLX1, EMX2, hASH1, NGN2 and OLIG2 compared to the expression of *PAX2*, *PAX5*, *PAX6* and *PAX8*. The amount of expression on mRNA level was measured by qPCR and evaluated according to Muratovska et al.[32] No correlation between the expression of PAX transcription factors and

homeobox or helix-loop-helix transcription factors were observed. Furthermore no correlation existed with p53 status according to Ishii et al.[53] (wt=wild-type; mt=mutant; nu=null).

Acknowledgements

The Dr. Senckenberg Institute of Neurooncology is supported by the Hertie foundation and the Dr. Senckenberg foundation. JS is “Hertie Professor for Neurooncology”. This work was supported by the graduate college 686-1 “Mechanismen der Entstehung solider Tumoren und experimentelle Therapie-Konzepte”.

References

1. Lang D, Powell SK, Plummer RS, Young KP, Ruggeri BA. PAX genes: Roles in development, pathophysiology, and cancer. Biochem Pharmacol 2006.
2. Walther C, Guenet JL, Simon D, et al. Pax: a murine multigene family of paired box-containing genes. Genomics 1991;11(2):424-34.
3. Chi N, Epstein JA. Getting your Pax straight: Pax proteins in development and disease. Trends Genet 2002;18(1):41-7.
4. Maulbecker CC, Gruss P. The oncogenic potential of Pax genes. Embo J 1993;12(6):2361-7.
5. Maulbecker CC, Gruss P. The oncogenic potential of deregulated homeobox genes. Cell Growth Differ 1993;4(5):431-41.
6. Stuart ET, Gruss P. PAX: developmental control genes in cell growth and differentiation. Cell Growth Differ 1996;7(3):405-12.
7. Urbanek P, Fetka I, Meisler MH, Busslinger M. Cooperation of Pax2 and Pax5 in midbrain and cerebellum development. Proc Natl Acad Sci U S A 1997;94(11):5703-8.
8. Goode DK, Elgar G. The PAX258 gene subfamily: a comparative perspective. Dev Dyn 2009;238(12):2951-74.
9. Morrison AM, Nutt SL, Thevenin C, Rolink A, Busslinger M. Loss- and gain-of-function mutations reveal an important role of BSAP (Pax-5) at the start and end of B cell differentiation. Semin Immunol 1998;10(2):133-42.
10. Dressler GR, Wilkinson JE, Rothenpieler UW, Patterson LT, Williams-Simons L, Westphal H. Deregulation of Pax-2 expression in transgenic mice generates severe kidney abnormalities. Nature 1993;362(6415):65-7.
11. Kozmik Z, Kurzbauer R, Dorfler P, Busslinger M. Alternative splicing of Pax-8 gene transcripts is developmentally regulated and generates isoforms with different transactivation properties. Mol Cell Biol 1993;13(10):6024-35.
12. St-Onge L, Sosa-Pineda B, Chowdhury K, Mansouri A, Gruss P. Pax6 is required for differentiation of glucagon-producing alpha-cells in mouse pancreas. Nature 1997;387(6631):406-9.
13. Sosa-Pineda B, Chowdhury K, Torres M, Oliver G, Gruss P. The Pax4 gene is essential for differentiation of insulin-producing beta cells in the mammalian pancreas. Nature 1997;386(6623):399-402.
14. Kozmik Z, Sure U, Ruedi D, Busslinger M, Aguzzi A. Deregulated expression of PAX5 in medulloblastoma. Proc Natl Acad Sci U S A 1995;92(12):5709-13.
15. Santisteban P, Bernal J. Thyroid development and effect on the nervous system. Rev Endocr Metab Disord 2005;6(3):217-28.
16. Stuart ET, Haffner R, Oren M, Gruss P. Loss of p53 function through PAX-mediated transcriptional repression. Embo J 1995;14(22):5638-45.
17. Barr FG, Galili N, Holick J, Biegel JA, Rovera G, Emanuel BS. Rearrangement of the PAX3 paired box gene in the paediatric solid tumour alveolar rhabdomyosarcoma. Nat Genet 1993;3(2):113-7.
18. Galili N, Davis RJ, Fredericks WJ, et al. Fusion of a fork head domain gene to PAX3 in the solid tumour alveolar rhabdomyosarcoma. Nat Genet 1993;5(3):230-5.
19. Shapiro DN, Sublett JE, Li B, Downing JR, Naeve CW. Fusion of PAX3 to a member of the forkhead family of transcription factors in human alveolar rhabdomyosarcoma. Cancer Res 1993;53(21):5108-12.
20. Busslinger M, Klix N, Pfeffer P, Graninger PG, Kozmik Z. Deregulation of PAX-5 by translocation of the Emu enhancer of the IgH locus adjacent to two alternative PAX-5 promoters in a diffuse large-cell lymphoma. Proc Natl Acad Sci U S A 1996;93(12):6129-34.

21. Iida S, Rao PH, Nallasivam P, et al. The t(9;14)(p13;q32) chromosomal translocation associated with lymphoplasmacytoid lymphoma involves the PAX-5 gene. Blood 1996;88(11):4110-7.
22. Kroll TG, Sarraf P, Pecciarini L, et al. PAX8-PPARgamma1 fusion oncogene in human thyroid carcinoma. Science 2000;289(5483):1357-60.
23. Murer L, Caridi G, Della Vella M, et al. Expression of nuclear transcription factor PAX2 in renal biopsies of juvenile nephronophthisis. Nephron 2002;91(4):588-93.
24. Winyard PJ, Risdon RA, Sams VR, Dressler GR, Woolf AS. The PAX2 tanscription factor is expressed in cystic and hyperproliferative dysplastic epithelia in human kidney malformations. J Clin Invest 1996;98(2):451-9.
25. Amiel J, Audollent S, Joly D, et al. PAX2 mutations in renal-coloboma syndrome: mutational hotspot and germline mosaicism. Eur J Hum Genet 2000;8(11):820-6.
26. Nishimoto K, Iijima K, Shirakawa T, et al. PAX2 gene mutation in a family with isolated renal hypoplasia. J Am Soc Nephrol 2001;12(8):1769-72.
27. Porteous S, Torban E, Cho NP, et al. Primary renal hypoplasia in humans and mice with PAX2 mutations: evidence of increased apoptosis in fetal kidneys of Pax2(1Neu) +/- mutant mice. Hum Mol Genet 2000;9(1):1-11.
28. Schimmenti LA, Cunliffe HE, McNoe LA, et al. Further delineation of renal-coloboma syndrome in patients with extreme variability of phenotype and identical PAX2 mutations. Am J Hum Genet 1997;60(4):869-78.
29. Gnarra JR, Dressler GR. Expression of Pax-2 in human renal cell carcinoma and growth inhibition by antisense oligonucleotides. Cancer Res 1995;55(18):4092-8.
30. Hueber PA, Waters P, Clark P, Eccles M, Goodyer P. PAX2 inactivation enhances cisplatin-induced apoptosis in renal carcinoma cells. Kidney Int 2006;69(7):1139-45.
31. Torban E, Eccles MR, Favor J, Goodyer PR. PAX2 suppresses apoptosis in renal collecting duct cells. Am J Pathol 2000;157(3):833-42.
32. Muratovska A, Zhou C, He S, Goodyer P, Eccles MR. Paired-Box genes are frequently expressed in cancer and often required for cancer cell survival. Oncogene 2003;22(39):7989-97.
33. Zhang SL, Guo J, Moini B, Ingelfinger JR. Angiotensin II stimulates Pax-2 in rat kidney proximal tubular cells: impact on proliferation and apoptosis. Kidney Int 2004;66(6):2181-92.
34. Steinbach JP, Kozmik Z, Pfeffer P, Aguzzi A. Overexpression of Pax5 is not sufficient for neoplastic transformation of mouse neuroectoderm. Int J Cancer 2001;93(4):459-67.
35. Ward TA, Nebel A, Reeve AE, Eccles MR. Alternative messenger RNA forms and open reading frames within an additional conserved region of the human PAX-2 gene. Cell Growth Differ 1994;5(9):1015-21.
36. McConnell MJ, Cunliffe HE, Chua LJ, Ward TA, Eccles MR. Differential regulation of the human Wilms tumour suppressor gene (WT1) promoter by two isoforms of PAX2. Oncogene 1997;14(22):2689-700.
37. Roth W, Fontana A, Trepel M, Reed JC, Dichgans J, Weller M. Immunochemotherapy of malignant glioma: synergistic activity of CD95 ligand and chemotherapeutics. Cancer Immunol Immunother 1997;44(1):55-63.
38. Steinbach JP, Klumpp A, Wolburg H, Weller M. Inhibition of epidermal growth factor receptor signaling protects human malignant glioma cells from hypoxia-induced cell death. Cancer Res 2004;64(5):1575-8.
39. Livak KJ, Schmittgen TD. Analysis of relative gene expression data using real-time quantitative PCR and the 2(-Delta Delta C(T)) Method. Methods 2001;25(4):402-8.
40. Steinbach JP, Wolburg H, Klumpp A, Probst H, Weller M. Hypoxia-induced cell death in human malignant glioma cells: energy deprivation promotes decoupling of

mitochondrial cytochrome c release from caspase processing and necrotic cell death. Cell Death Differ 2003;10(7):823-32.
41. Louis DN, Ohgaki H, Wiestler OD, et al. The 2007 WHO classification of tumours of the central nervous system. Acta neuropathologica 2007;114(2):97-109.
42. Liao CL, Lee MY, Tyan YS, et al. Progesterone receptor does not improve the performance and test effectiveness of the conventional 3-marker panel, consisting of estrogen receptor, vimentin and carcinoembryonic antigen in distinguishing between primary endocervical and endometrial adenocarcinomas in a tissue microarray extension study. Journal of translational medicine 2009;7:37.
43. Zhou YH, Wu X, Tan F, et al. PAX6 suppresses growth of human glioblastoma cells. J Neurooncol 2005;71(3):223-9.
44. Ronellenfitsch MW, Brucker DP, Burger MC, et al. Antagonism of the mammalian target of rapamycin selectively mediates metabolic effects of epidermal growth factor receptor inhibition and protects human malignant glioma cells from hypoxia-induced cell death. Brain 2009;132(Pt 6):1509-22.
45. Brophy PD, Ostrom L, Lang KM, Dressler GR. Regulation of ureteric bud outgrowth by Pax2-dependent activation of the glial derived neurotrophic factor gene. Development 2001;128(23):4747-56.
46. Phillips HS, Kharbanda S, Chen R, et al. Molecular subclasses of high-grade glioma predict prognosis, delineate a pattern of disease progression, and resemble stages in neurogenesis. Cancer Cell 2006;9(3):157-73.
47. Bouchard M, Pfeffer P, Busslinger M. Functional equivalence of the transcription factors Pax2 and Pax5 in mouse development. Development 2000;127(17):3703-13.
48. Bouchard M, de Caprona D, Busslinger M, Xu P, Fritzsch B. Pax2 and Pax8 cooperate in mouse inner ear morphogenesis and innervation. BMC developmental biology;10:89.
49. Schwarz M, Cecconi F, Bernier G, et al. Spatial specification of mammalian eye territories by reciprocal transcriptional repression of Pax2 and Pax6. Development 2000;127(20):4325-34.
50. Scholl FA, Kamarashev J, Murmann OV, Geertsen R, Dummer R, Schafer BW. PAX3 is expressed in human melanomas and contributes to tumor cell survival. Cancer Res 2001;61(3):823-6.
51. He SJ, Stevens G, Braithwaite AW, Eccles MR. Transfection of melanoma cells with antisense PAX3 oligonucleotides additively complements cisplatin-induced cytotoxicity. Molecular cancer therapeutics 2005;4(6):996-1003.
52. Gibson W, Green A, Bullard RS, Eaddy AC, Donald CD. Inhibition of PAX2 expression results in alternate cell death pathways in prostate cancer cells differing in p53 status. Cancer Lett 2007;248(2):251-61.
53. Ishii N, Maier D, Merlo A, et al. Frequent co-alterations of TP53, p16/CDKN2A, p14ARF, PTEN tumor suppressor genes in human glioma cell lines. Brain pathology 1999;9(3):469-79.

Fig. 1

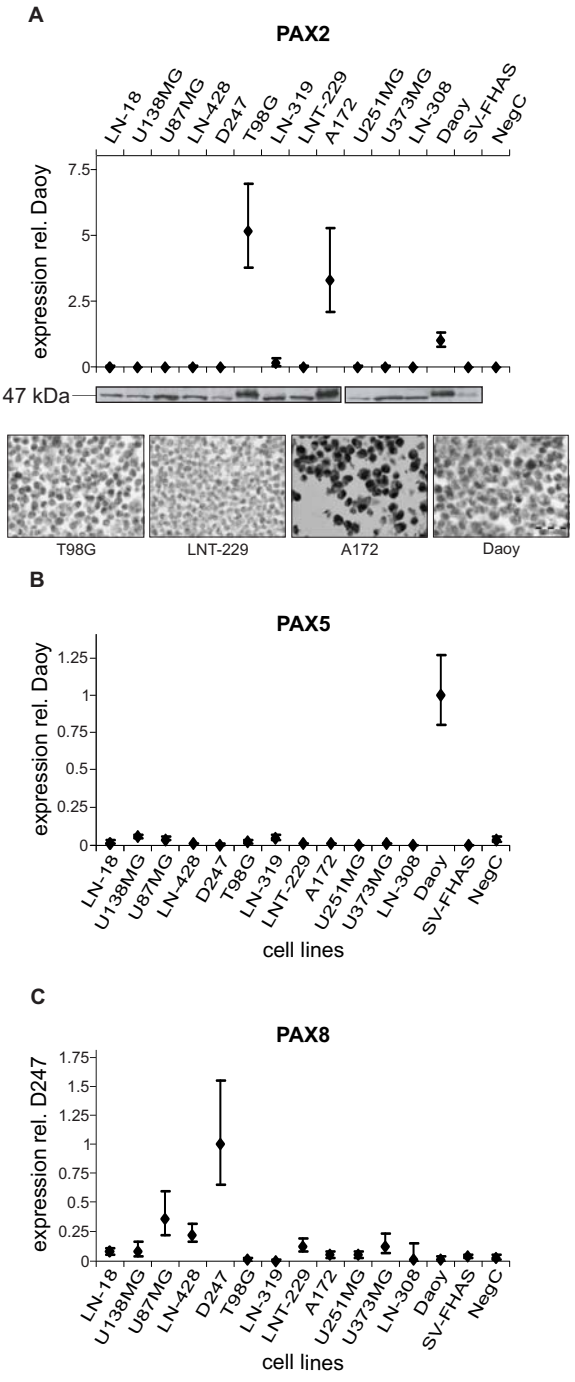
A
PAX2
LN-18
U138MG
U87MG
LN-428
D247
T98G
LN-319
LNT-229
A172
U251MG
U373MG
LN-308
Daoy
SV-FHAS
NegC
expression rel. Daoy
7.5
5
2.5
0
47 kDa
T98G
LNT-229
A172
Daoy
B
PAX5
expression rel. Daoy
1.25
1
0.75
0.5
0.25
0
cell lines
C
PAX8
expression rel. D247
1.75
1.5
1.25
1
0.75
0.5
0.25
0
cell lines

Fig. 2

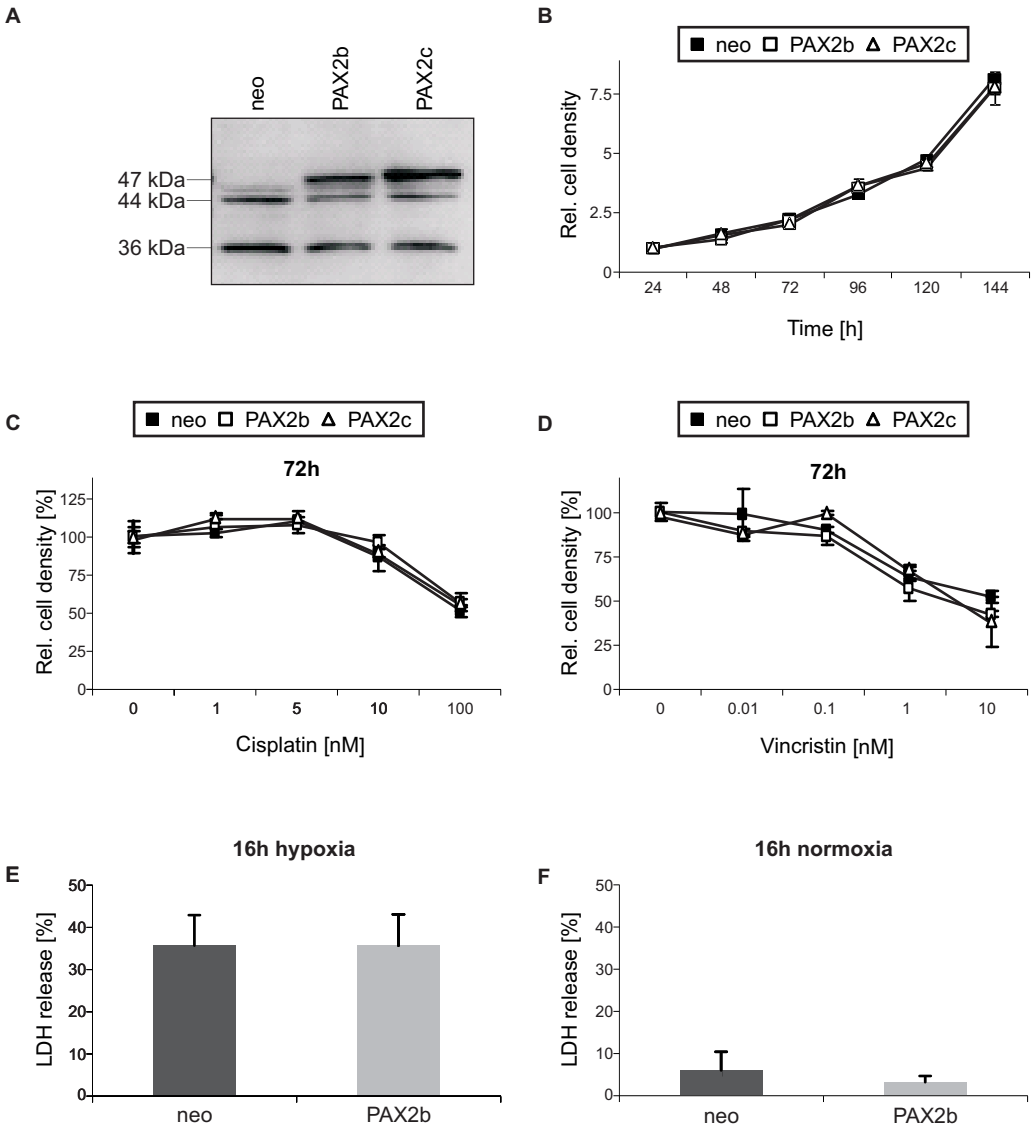
A
neo
PAX2b
PAX2c
47 kDa
44 kDa
36 kDa
B
neo PAX2b PAX2c
Rel. cell density
Time [h]
C
neo PAX2b PAX2c
72h
Rel. cell density [%]
Cisplatin [nM]
D
neo PAX2b PAX2c
72h
Rel. cell density [%]
Vincristin [nM]
E
16h hypoxia
LDH release [%]
neo
PAX2b
F
16h normoxia
LDH release [%]
neo
PAX2b

Fig. 3

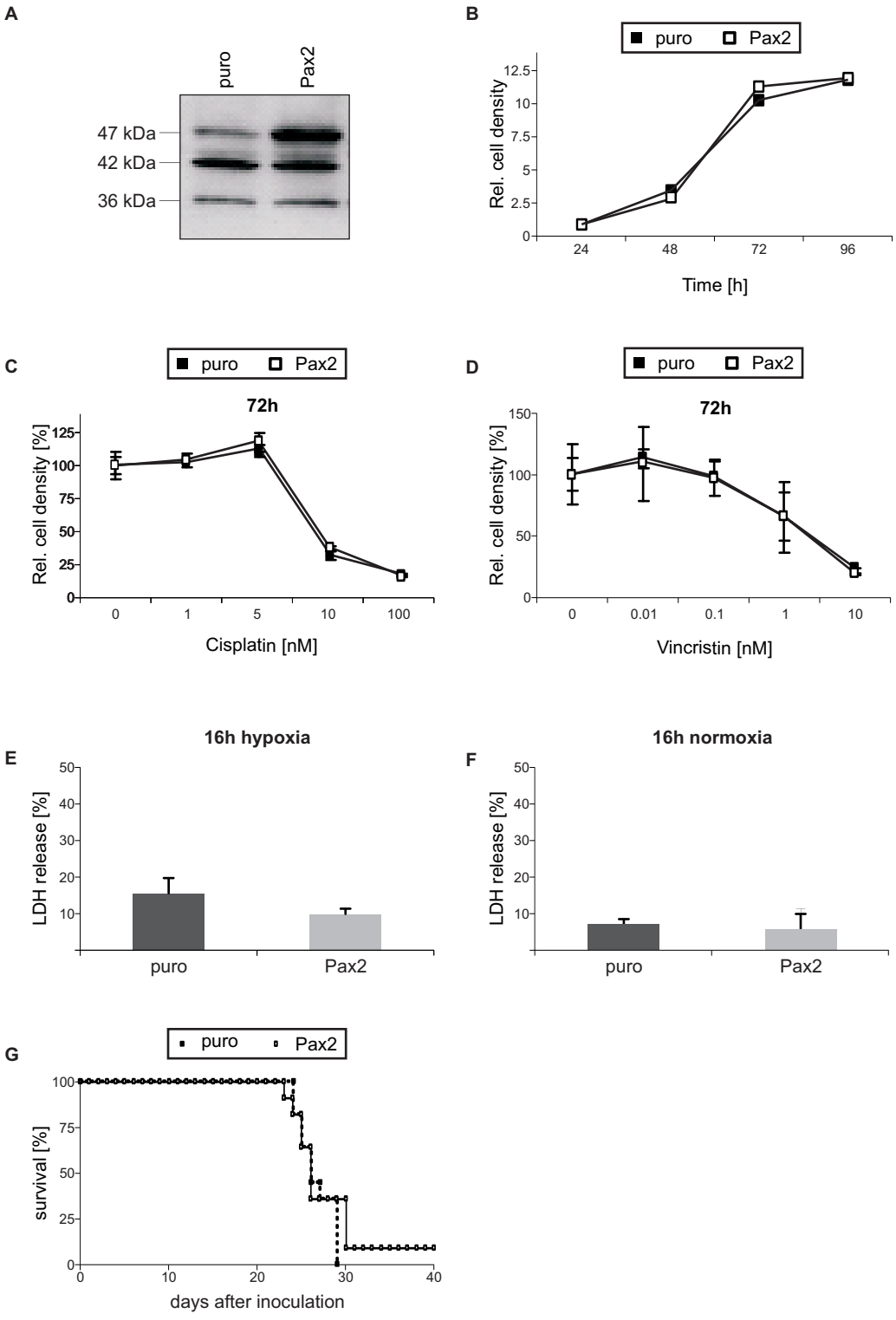
A
puro
Pax2
47 kDa
42 kDa
36 kDa
B
puro
Pax2
Rel. cell density
12.5
10
7.5
5
2.5
0
24
48
72
96
Time [h]
C
puro
Pax2
72h
Rel. cell density [%]
125
100
75
50
25
0
0
1
5
10
100
Cisplatin [nM]
D
puro
Pax2
72h
Rel. cell density [%]
150
100
50
0
0
0.01
0.1
1
10
Vincristin [nM]
E
16h hypoxia
LDH release [%]
50
40
30
20
10
puro
Pax2
F
16h normoxia
LDH release [%]
50
40
30
20
10
puro
Pax2
G
puro
Pax2
survival [%]
100
75
50
25
0
0
10
20
30
40
days after inoculation

Fig. 4

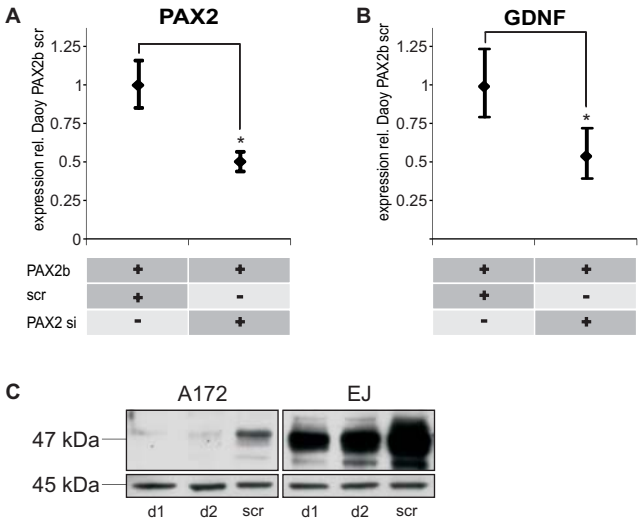
A
PAX2
expression rel. Daoy PAX2b scr
1.25
1
0.75
0.5
0.25
0
*
PAX2b
scr
PAX2 si
B
GDNF
expression rel. Daoy PAX2b scr
1.25
1
0.75
0.5
0.25
*

C
A172
EJ
47 kDa
45 kDa
d1
d2
scr
d1
d2
scr

Fig. 5

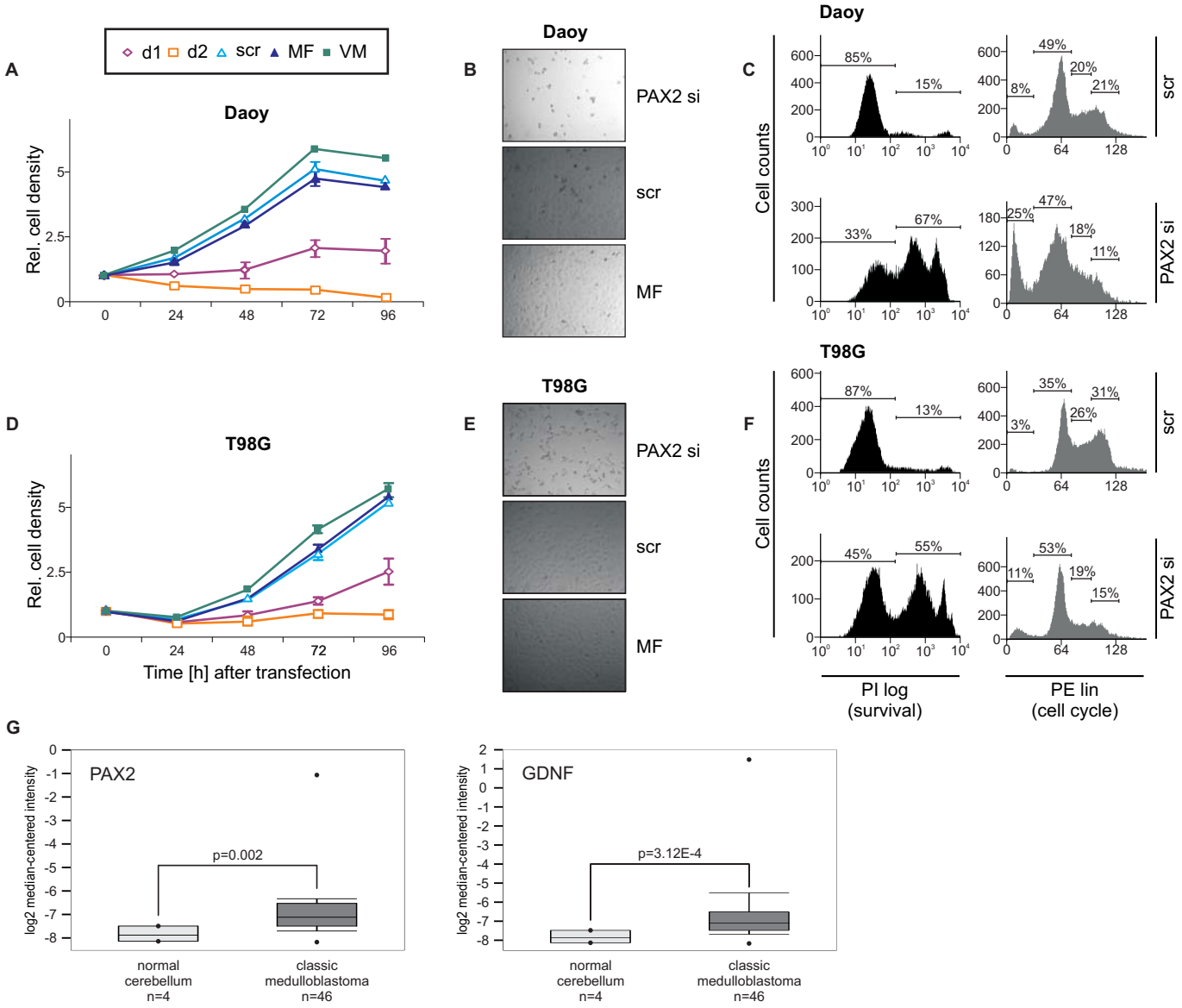
A
d1 d2 scr MF VM
Daoy
Rel. cell density
Time [h] after transfection
B
Daoy
PAX2 si
scr
MF
C
Daoy
Cell counts
scr
PAX2 si
D
T98G
E
T98G
F
T98G
PI log
(survival)
PE lin
(cell cycle)
G
PAX2
p=0.002
GDNF
p=3.12E-4
log2 median-centered intensity
normal
cerebellum
n=4
classic
medulloblastoma
n=46

Fig. 6

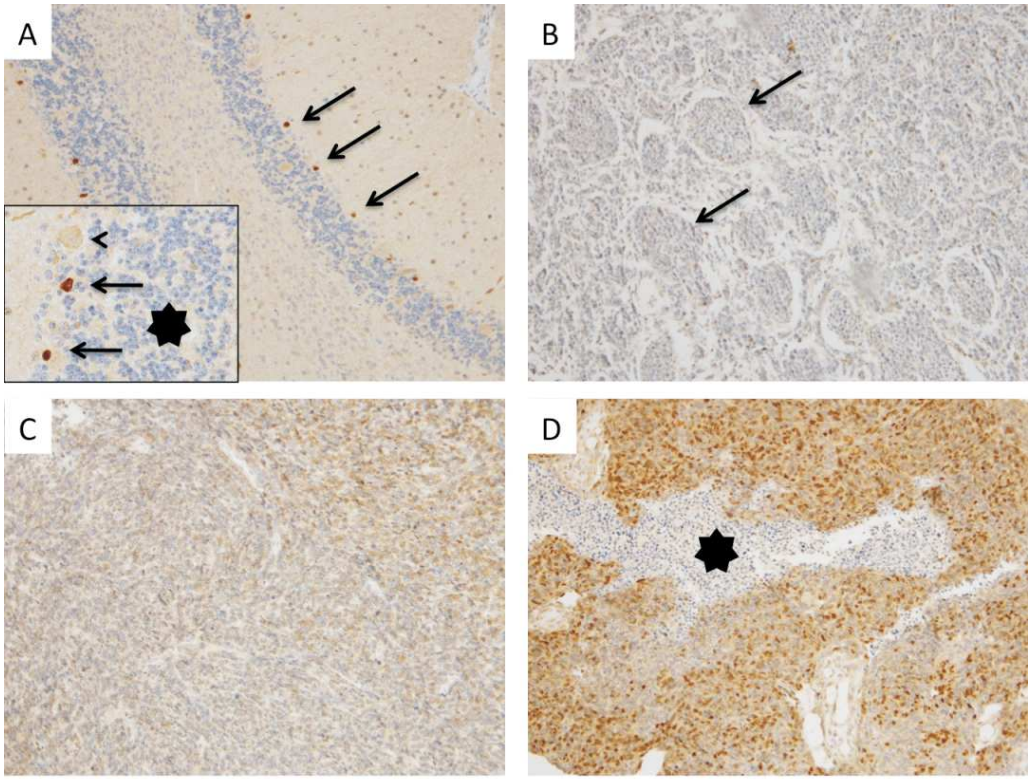
A
B
C
D

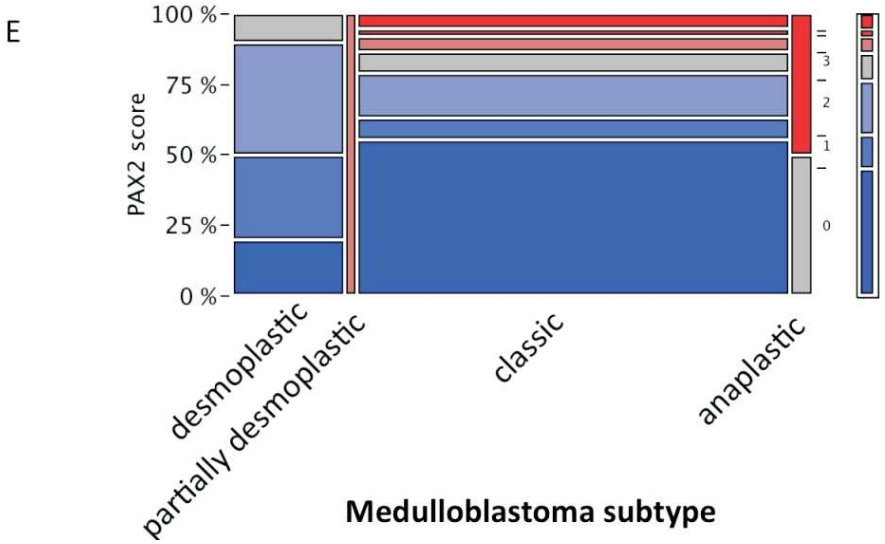
E
100 %
75 %
50 %
25 %
0 %
PAX2 score
3
2
1
0
desmoplastic
partially desmoplastic
classic
anaplastic
Medulloblastoma subtype

Table 1

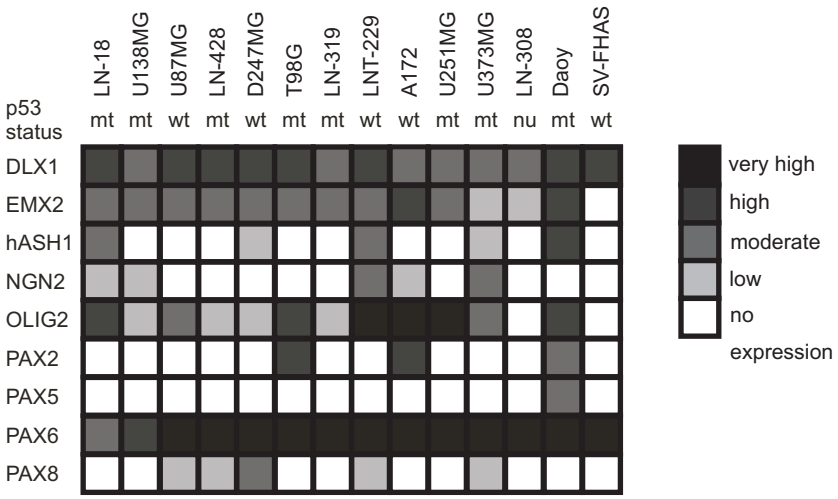
LN-18
U138MG
U87MG
LN-428
D247MG
T98G
LN-319
LNT-229
A172
U251MG
U373MG
LN-308
Daoy
SV-FHAS
p53 status
mt mt wt mt wt mt mt wt wt mt mt nu mt wt
DLX1
EMX2
hASH1
NGN2
OLIG2
PAX2
PAX5
PAX6
PAX8
very high
high
moderate
low
no expression